A Method for Tractable Dynamical Studies of Single and Double Shock Compression

Evan J. Reed,[1,*] Laurence E. Fried,[2] and J. D. Joannopoulos[1]

[1]*Department of Physics, Massachusetts Institute of Technology, Cambridge, Massachusetts 02139, USA*

[2]*Chemistry and Materials Science Directorate, Lawrence Livermore National Laboratory, Livermore, California 94550, USA*

(Received 4 December 2002; published 13 June 2003)

A new multiscale simulation method is formulated for the study of shocked materials. The method combines molecular dynamics and the Euler equations for compressible flow. Treatment of the difficult problem of the spontaneous formation of multiple shock waves due to material instabilities is enabled with this approach. The method allows the molecular dynamics simulation of the system under dynamical shock conditions for orders of magnitude longer time periods than is possible using the popular nonequilibrium molecular dynamics approach. An example calculation is given for a model potential for silicon in which a computational speedup of 10^5 is demonstrated. Results of these simulations are consistent with the recent experimental observation of an anomalously large elastic precursor on the nanosecond time scale.

DOI: 10.1103/PhysRevLett.90.235503 PACS numbers: 62.50.+p, 46.40.Cd, 82.40.Fp

Study of the propagation of shock waves in condensed matter has led to new discoveries ranging from new metastable states of carbon [1] to the metallic conductivity of hydrogen in Jupiter [2,3], but progress in understanding the microscopic details of shocked materials has been extremely difficult. Highly nonequilibrium regions may exist that give rise to the formation of unexpected metastable states of matter and determine the structure, instabilities, and time evolution of the shock wave [4–7]. Some progress in understanding these microscopic details can be made through molecular dynamics simulations [8–11]. The popular nonequilibrium molecular dynamics (NEMD) approach to atomistic simulations of shock compression involves creating a shock on one edge of a large system and allowing it to propagate until it reaches the other side. The computational work required by NEMD scales at least quadratically in the evolution time because larger systems are needed for longer simulations. When quantum mechanical methods with poor scaling of computational effort with system size are employed, this approach to shock simulations rapidly becomes impossible. Another approach that utilizes a computational cell moving at the shock speed has the same drawbacks [12]. This Letter presents a method that circumvents these difficulties by requiring simulation of only a small part of the entire system. The effects of the shock wave passing through this small piece of the system are simulated by dynamically regulating the applied stress which is obtained from a continuum theory description of the shock wave structure. Because the size of the molecular dynamics system is independent of the simulation time in this approach, the computational work required to simulate a shocked system is nearly linear in the simulation time, circumventing the scaling problems of NEMD.

Molecular dynamics simulations have been performed that utilize a shock Hugoniot-based thermodynamic constraint for the temperature at fixed volume [13]. This approach is a thermodynamic one for a single shock wave and fails to capture the spontaneous formation of multiple shock waves and dynamical effects such as long-lived metastable phases, elastic-plastic phase transitions, and chemical reactions, which are ubiquitous in shocked condensed matter. The new method outlined in this Letter solves these problems. It enables the *dynamical* simulation of shock waves in systems that have material instabilities which lead to the formation of multiple shock waves and chemical reactions that can change the speed of shock propagation with time. It is a tractable method that requires no *a priori* knowledge of the system phase diagram, metastable states, or sound speeds.

Method for simulation of a single shock wave.—We model the propagation of the shock wave using the 1D Euler equations for compressible flow, which neglect thermal transport. These equations represent the conservation of mass, momentum, and energy, respectively, everywhere in the wave. Neglecting thermal transport in high-temperature shocks is valid in systems where electronic mechanisms of heat conduction are not important, i.e., usually less than a few thousand K in insulators [14]. While the Euler equations are not rigorously applicable at elastic shock fronts which can be atomistically sharp, the correct dynamics will be approximated in these special regions. We seek solutions of these equations which are steady in the frame of the shock wave moving at speed v_s by making the substitution $(x, t) \rightarrow x - v_s t$. This substitution and integration over x yields a variation of the Hugoniot relations,

$$u = v_s\left(1 - \frac{\rho_0}{\rho}\right), \tag{1}$$

$$p - p_0 = v_s^2 \rho_0\left(1 - \frac{\rho_0}{\rho}\right), \tag{2}$$

$$e - e_0 = p_0\left(\frac{1}{\rho_0} - \frac{1}{\rho}\right) + \frac{v_s^2}{2}\left(1 - \frac{\rho_0}{\rho}\right)^2. \quad (3)$$

Here u is the local speed of the material in the laboratory frame (particle velocity), v is the specific volume, $\rho = 1/v$ is the density, e is the energy per unit mass, and p is the negative component of the stress tensor in the direction of shock propagation, $-\sigma_{xx}$. Variables with subscript 0 are the values before the shock wave, and we have chosen $u_0 = 0$, i.e., the material is initially at rest in the laboratory frame. In the language of shock physics, Eq. (2) for the pressure is the Rayleigh line and Eq. (3) for the internal energy is the Hugoniot at constant shock velocity. These equations apply to a system which has a time-independent steady state in the reference frame moving at the shock speed v_s.

For the molecular dynamics simulation, we employ the Lagrangian,

$$L = T(\{\dot{\vec{r}}_i\}) - V(\{\vec{r}_i\}) + \frac{1}{2}Q\dot{v}^2 + \frac{1}{2}\frac{v_s^2}{v_0^2}(v_0 - v)^2 + p_0(v_0 - v), \quad (4)$$

where T and V are kinetic and potential energies per unit mass, and Q is a masslike parameter for the simulation cell size. It can be seen that Eq. (4) in Hamiltonian form implies Eq. (3) when $\dot{v} = 0$ because $T + V = e$. The equation of motion for the system volume is

$$Q\ddot{v} = \frac{\partial T}{\partial v} - \frac{\partial V}{\partial v} - p_0 - \frac{v_s^2}{v_0^2}(v_0 - v), \quad (5)$$

which reduces to Eq. (2) when $\ddot{v} = 0$. We use the scaled atomic coordinate scheme of Ref. [15] to deal with the variable computational cell size. This scheme introduces a volume dependence for T and V. Strain is allowed only in the shock direction, i.e., $v_0 - v = -\epsilon_{xx}v_0$ where ϵ_{xx} is the uniaxial strain. The pressures in Eq. (5), including the thermal contribution, are taken to be the uniaxial x component of stresses. Computational cell dimensions transverse to the shock direction are fixed, as in NEMD simulations. This approach allows the simulation of shocks propagating in any direction which is difficult or impossible with NEMD.

Simulation of a single shock wave may be accomplished by dynamically varying the uniaxial strain of the system according to Eq. (5). By choosing a small representative sample of the shocked material, it is assumed that stress gradients and thermal gradients in the actual shock wave are negligible on the length scale of the sample size. While the thermal energy is assumed to be evenly distributed throughout the sample, thermal equilibrium is not required.

To simulate a shock to a given pressure, the initial state parameters which define the molecular dynamics constraint in Eq. (4) are chosen (ρ_0, p_0, e_0). A guess for v_s is made for the constraint to take the system to the desired final pressure. If the final pressure is other than the desired one, improved guesses for v_s can be made and simulated again until the desired v_s is determined. The final shock pressure increases with increasing v_s. The simulation of a shock to a given particle velocity using this approach is a straightforward extension.

Stability of simulated waves.—There are two criteria for the mechanical stability of a shock wave [16]. The first one requires $v_s > c_0$, where c_0 is the speed of sound in the preshocked material. The second criterion requires $u_1 + c_1 > v_s$, where the subscript 1 denotes the postshock state.

The constraints of Eqs. (2) and (3) take the system through states which satisfy these stability criteria. The line between points A and E in Fig. 1 depicts a Rayleigh line for a single shock on a Hugoniot. Points A and E are stationary points of Eq. (5). The Rayleigh line slope magnitude must be greater than the Hugoniot slope at point A to be an unstable stationary point of Eq. (5) and vice versa at point E to be a stable point of Eq. (5). These conditions are required for the compression to proceed up along the Rayleigh line.

The Hugoniot and isentrope have a first-order tangent at point A. Therefore, the stability condition $c_0 < v_s$ is automatically satisfied at point A if compression proceeds up along the Rayleigh line, since the Rayleigh line slope is $-(v_s^2/v_0^2)$ and the Hugoniot slope is $-(c_0^2/v_0^2)$. Furthermore, since the Rayleigh line slope magnitude is less than the Hugoniot slope at point E, it can be shown that $u_1 + c_1 > v_s$, which is the other stability condition. Therefore, the constraint Eq. (5) has stable points only where the shock waves are stable.

Treatment of multiple shock waves.—The above method describes the simulation of a single stable shock wave. However, it is not always possible to shock to a given pressure or particle velocity using this technique. For example, Fig. 1 shows how it may not be possible to connect a straight Rayleigh line to all final pressures when there is a region of negative curvature in the Hugoniot, $d^2p/dv^2 < 0$. Such regions of negative curvature are common in condensed phase materials and may be a result of phase transformations or may be the shape of a single phase Hugoniot. In Fig. 1, it is not possible to

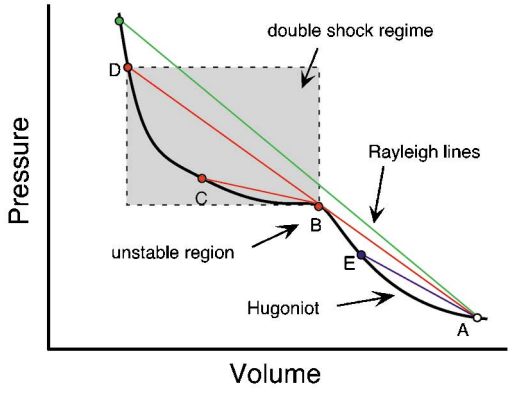

FIG. 1 (color). Rayleigh lines on a hypothetical Hugoniot.

connect state A to any state between B and D with a straight Rayleigh line. Therefore, it is not possible for a single shock wave to compress the system to a pressure between that of states B and D. While a single Rayleigh line is insufficient to meet the pressure boundary condition in this region, two Rayleigh lines are sufficient. The first goes from A to B and is tangent to the Hugoniot at point B. This tangency implies $u_B + c_B = v_{s,AB}$ at point B which is a point of instability. Therefore, the wave from A to B terminates and a second wave forms from B to C. The mechanical stability criteria are satisfied at points A and C.

Figure 2 shows a flowchart that illustrates how to determine the set of Rayleigh lines that are stable and meet the boundary conditions without any *a priori* knowledge of the system. A shock wave instability exists when the boundary condition falls within a discontinuity in the set of final pressures as a function of shock speed, as in the inset in Fig. 2. The existence of such a discontinuity can be determined when sufficient trial values of v_s have been simulated. If the boundary condition falls within the discontinuity, the entire process is repeated with point B as the initial state to find the shock speed that meets the boundary condition. If further instabilities are discovered that prevent the boundary condition from being met with a single shock, the process is continued.

Time dependence of the p-v space path.—The formation and evolution of multiple waves becomes more complicated when chemical reactions or phase transitions occur. Volume decreasing phase transformations cause the pressure at point B in Figs. 1 and 2 to decrease with time. Parametrization of the p-v space path with Rayleigh lines is valid when the time scale of this pressure change is less than the time required for a material element to reach the final shocked state.

The rate at which the pressure at point B decreases can be determined using the shock change equation [17,18]. If we assume the internal energy is $e = e(p, v, \lambda)$, where λ is the reaction parameter for the phase transition, then the rate of pressure change in the moving frame of the shock wave at the metastable point B is given by

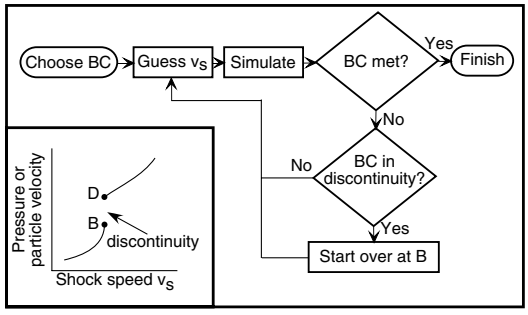

FIG. 2. Flowchart for simulation of a shock to a chosen pressure or particle velocity boundary condition. Instabilities due to regions where $d^2p/dv^2 < 0$ along the Hugoniot can give rise to a discontinuity in the inset plot.

$$\left.\frac{dp}{dt}\right|_{v_s} = \frac{\rho(u - v_s)^2 \alpha \dot{\lambda}}{2}. \tag{6}$$

Here λ ranges between 0 and 1, $\alpha = \rho \frac{\partial v}{\partial \lambda}|_{p,H}$, where H is the enthalpy, and we have made use of the fact that $v_s - u = c = \sqrt{(\partial p/\partial \rho)|_{s,\lambda}}$ and $\frac{\partial u}{\partial p}|_{\text{Hugoniot}} = \frac{\partial u}{\partial p}|_{\text{Rayleigh}} = \frac{1}{\rho_0 v_s}$ at the point of instability where the Hugoniot and Rayleigh lines share a common tangent. We take the parameter $\alpha\dot{\lambda}$ to be $\frac{\delta v}{v \delta t}$, where δt is the time required for a volume change δv at the start of chemistry or plastic deformation, which is taken to be the point where the rate of simulation compression is slowest.

The approximation of the p-v space path by more than one Rayleigh line in the case of volume decreasing reactions is justified when the Rayleigh lines do not change appreciably during the simulation,

$$\left.\frac{dp}{dt}\right|_{v_s} \ll \frac{\Delta p}{\Delta t}, \tag{7}$$

where Δp and Δt are the pressure change and time duration of a given simulation, respectively. In a two-shock wave, the time the system spends going from the initial state to the final state Δt is a function of the shock speeds associated with each wave and is linear in time and the difference between wave speeds. In the long time limit, $\frac{dp}{dt}|_{v_s}$ decreases exponentially with time [16]. Therefore, the Rayleigh line validity condition is satisfied in the long simulation time limit. During times when this condition is not satisfied, the p-v space path that a material element follows is more complicated than straight Rayleigh lines, but such situations are transient.

Application to silicon.—As an illustrative example, we apply the new method to an elastic-plastic transition in a model potential for silicon. Figure 3 shows shock speed as a function of particle velocity for shock waves propagating in the [011] direction in silicon described by the Stillinger-Weber potential [19]. This potential has been found to provide a qualitative representation of condensed properties of silicon. Data calculated using the NEMD method are compared with results of the new method presented in this Letter. NEMD simulations were done with a computational cell of size 920 Å $\times$ 12 Å $\times$ 11 Å ($240 \times 3 \times 2$ unit cells, or 5760 atoms) for a duration of about 10–20 ps. Simulations with the new method were done with a computational cell size of 19 Å $\times$ 12 Å $\times$ 11 Å ($5 \times 3 \times 2$ unit cells, or 120 atoms). Both simulations were started at 300 K and zero stress. Since the NEMD simulations were limited to the 10 ps time scale by computational cost, simulations with the new method were performed to calculate the Hugoniot on this 10 ps time scale for comparison. The final particle velocity in these simulations was taken to be a point of steady state after a few picoseconds. The Rayleigh line validity condition Eq. (7) is satisfied for the simulations performed in the two-shock regime, giving a typical value for $\frac{dp}{dt}|_{v_s}$ of

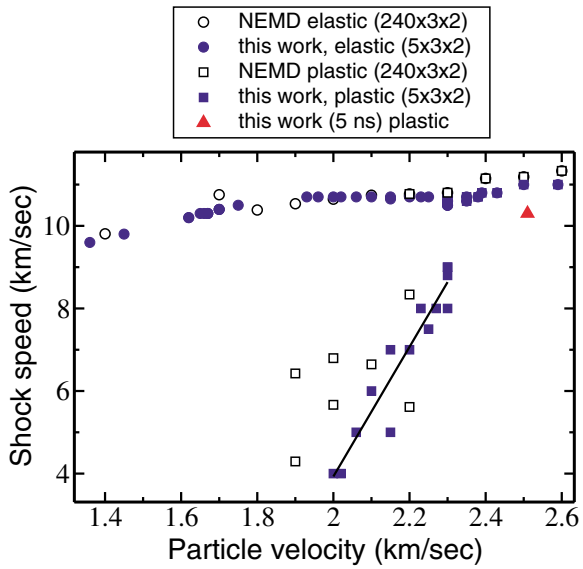

FIG. 3 (color). Comparison of calculated Hugoniots for the NEMD approach and the method presented in this Letter for roughly 10 ps runs. Note the ability to utilize much smaller computational cell sizes with the new method. Also included is one data point for a 5 ns simulation using this work which would be prohibitive with NEMD requiring a factor of 10^5 increase in computational effort.

0.1 GPa/ps, while $\frac{\Delta p}{\Delta t}$ is always greater than 0.5 GPa/ps for all simulations in Fig. 3.

Figure 3 indicates that a single shock wave exists below 1.9 km/sec particle velocity. Above this particle velocity, an elastic shock wave precedes a slower moving shock characterized by plastic deformation. Agreement between the two methods is good for all regions except for the plastic wave speed for particle velocities less than 2.1 km/sec. The wide range of values for the plastic wave speeds in NEMD simulations in this regime is due to finite simulation cell size effects. Better agreement in this regime can be obtained by using simulation cells with larger cross sectional area.

One of the primary advantages of using the method outlined in this Letter is the ability to simulate for much longer times than is possible with NEMD. As an example, Fig. 3 shows the result of a 5 ns simulation performed along a Rayleigh line corresponding to a shock speed of 10.3 km/sec. The uniaxially compressed elastic state required 5 ns to undergo plastic deformation. The difference in particle velocity between the 10 ps and 5 ns simulations at this shock speed is 0.8 km/sec, suggesting that the elastically compressed state is metastable with an anomalously large lifetime. This is consistent with experimental observations of shocked silicon that indicate an anomalously high pressure elastic wave exists on the nanosecond time scale [5]. In addition to the simulations performed with the Stillinger-Weber potential, we have performed more accurate tight-binding [20] 120 atom simulations using the method of this Letter that also suggest an anomalously high pressure elastic wave precursor exists on the 10 ps time scale.

The 5 ns simulation done with NEMD would require *more* than 5 ns simulation time due to the time required for the equilibration of the first and second wave speeds according to Eq. (6). For an $\mathcal{O}(\mathcal{N})$ method of force evaluation, the computational cost of this simulation with the NEMD method would be at least 10^5 times greater and, therefore, not tractable.

We thank J. Forbes, C. Tarver, and D. Hare for helpful discussions. This work was performed under the auspices of the U.S. Department of Energy by the University of California, LLNL under Contract No. W-7405-Eng-48.

*Electronic address: evan@mit.edu

[1] C. S. Yoo, W. J. Nellis, M. L. Sattler, and R. G. Musket, Appl. Phys. Lett. **61**, 273 (1992).
[2] W. J. Nellis, S. T. Weir, and A. C. Mitchell, Science **273**, 936 (1996).
[3] S. T. Weir, A. C. Mitchell, and W. J. Nellis, Phys. Rev. Lett. **76**, 1860 (1996).
[4] M. D. Knudson and Y. M. Gupta, Phys. Rev. Lett. **81**, 2938 (1998).
[5] A. Loveridge-Smith *et al.*, Phys. Rev. Lett. **86**, 2349 (2001).
[6] A. Tokmakoff, M. D. Fayer, and D. D. Dlott, J. Phys. Chem. **97**, 1901 (1993).
[7] E. J. Reed, J. D. Joannopoulos, and L. E. Fried, Phys. Rev. B **62**, 16 500 (2000).
[8] K. Kadau, T. C. Germann, P. S. Lomdahl, and B. L. Holian, Science **296**, 1681 (2002).
[9] T. C. Germann, B. L. Holian, P. S. Lomdahl, and R. Ravelo, Phys. Rev. Lett. **84**, 5351 (2000).
[10] J. D. Kress, S. R. Bickham, L. A. Collins, B. L. Holian, and S. Goedecker, Phys. Rev. Lett. **83**, 3896 (1999).
[11] B. L. Holian and P. S. Lohmdahl, Science **280**, 2085 (1998).
[12] V. V. Zhakhovskiĭ, S. V. Zybin, K. Nishihara, and S. I. Anisimov, Phys. Rev. Lett. **83**, 1175 (1999).
[13] J. B. Maillet, M. Mareschal, L. Soulard, R. Ravelo, P. S. Lomdahl, T. C. Germann, and B. L. Holian, Phys. Rev. E **63**, 016121 (2001).
[14] Y. B. Zel'dovich and Y. P. Raizer, *Physics of Shock Waves and High-Temperature Hydrodynamic Phenomena* (Academic Press, New York, 1967).
[15] M. P. Allen and D. J. Tildesley, *Computer Simulation of Liquids* (Oxford University Press, New York, 1989).
[16] G. E. Duvall, in *Proceedings of the International School of Physics, Physics of High Energy Density* (Academic Press, New York, 1971), p. 7.
[17] E. Jouget, *Mecanique des Explosifs* (Octave Doin et Fils, Paris, 1917).
[18] W. Fickett and W. Davis, *Detonation* (University of California Press, Berkeley, CA, 1979).
[19] F. H. Stillinger and T. A. Weber, Phys. Rev. B **31**, 5262 (1985).
[20] S. Sawada, Vacuum **41**, 612 (1990).